Brownian motion of free particles on curved surfaces

Ramón Castañeda-Priego[(1)],* Pavel Castro-Villarreal[(2)],† Sendic Estrada-Jiménez[(2)],‡ and José Miguel Méndez-Alcaraz[(3)]§

[(1)] *División de Ciencias e Ingenierías, Campus León, Universidad de Guanajuato, Loma del Bosque 103, 37150 León, Guanajuato, Mexico*

[(2)] *Centro de Estudios en Física y Matemáticas Básicas y Aplicadas, Universidad Autónoma de Chiapas, Carretera Emiliano Zapata, Km. 8, Rancho San Francisco, C. P. 29050, Tuxtla Gutiérrez, Chiapas, Mexico and*

[(3)] *Departamento de Física, Cinvestav, Av. IPN 2508, Col. San Pedro Zacatenco, 07360 México, D. F., Mexico*

Brownian motion of free particles on curved surfaces is studied by means of the Langevin equation written in Riemann normal coordinates. In the diffusive regime we find the same physical behavior as the one described by the diffusion equation on curved manifolds [J. Stat. Mech. (2010) P08006]. Therefore, we use the latter in order to analytically study the whole diffusive dynamics in compact geometries, namely, the circle and the sphere. Our findings are corroborated by means of Brownian dynamics computer simulations based on a heuristic adaptation of the Ermak-McCammon algorithm to the Langevin equation along curves, as well as on the standard algorithm, but for particles perpendicularly attached to the surface through highly stiff springs. The short-time diffusive dynamics is found to occur on the tangential plane. Besides, at long times and compact geometries, the mean-square displacement moves towards a saturation value given only by the geometrical properties of the surface.

PACS numbers: 05.40.-a, 83.10.Mj, 82.70.-y

I. INTRODUCTION

Diffusive processes occur in a wide diversity of physical areas; ranging from soft condensed matter to particle physics and astrophysics [1–3]. In the latter case, such processes are relevant within the framework of special and general relativity (see, e.g., Ref. [4] and references therein). Furthermore, in the last few decades, an intense activity has emerged in biophysics to study protein diffusion on curved surfaces [5].

The transport phenomena of proteins occurring inside cell membranes are interesting and complex since they determine the flux of nutrients between the cell and its exterior affecting, in consequence, the cell functionality [6]. From the theoretical point of view, it is difficult to describe the lateral diffusion of integral proteins or lipids mainly because the interactions with the remaining components of the membrane and the protein finite-size effects [7, 8]. In addition, there are membrane curvature contributions [9] and thermal fluctuations that produce shape undulations in the membrane and, thus, have a crucial contribution to the transport phenomena. Furthermore, the coupling between lateral motion of proteins and thermal shape fluctuations has been recently considered by Reister and Seifert [10], whereas protein effects on the shape of the membrane surface were studied in references [11, 12]. Protein diffusion is also affected when changes in the membrane thickness are present [13, 14]. The study of protein lateral diffusion has been made possible by assuming the membrane as a two-dimensional regular and curved sheet and projecting the Smoluchowski equation on such a surface [9, 15–21]. In this approximation, both thermal shape fluctuations and finite-size effects have not been taken into account explicitly.

Recently, one of us explored the curvature effects on the Brownian motion, at short times, of free particles when their movement takes place in a d-dimensional Riemannian manifold [22]. In that work, a general method is provided to derive all moments, $\langle s^n \rangle$, of the probability density, $P(x, x', t)$, of finding a particle at a point x and time t when it started its movement at x'. In particular, the method is shown in which the mean-square displacement (MSD) is deviated from the planar expression by curvature terms which are $O(d)$-invariant, as well as invariant under general coordinate transformations. Here, s is the geodesic distance in the d-dimensional Riemannian manifold and $\langle \cdots \rangle$ stands for an ensemble average. It is also found that the second moment, up to second order in t, is given by [22]

$$\left\langle s^2 \right\rangle = 2dD_0 t - \frac{2}{3} R_g \left(D_0 t\right)^2 + \cdots , \tag{1}$$

where R_g is the Ricci scalar curvature of the general Riemannian manifold and D_0 is the free-particle diffusion coefficient. It is noteworthy to mention that the same curvature effects have also been explored to discuss the role of diffusion within the general relativity context [23].

Although the diffusion equation is suited to study the Brownian motion of free particles on curved surfaces [22], a more complete description is provided by the

*Electronic address: ramoncp@fisica.ugto.mx
†Electronic address: pcastrov@unach.mx
‡Electronic address: sestrada@unach.mx
§Electronic address: jmendez@fis.cinvestav.mx

Langevin equation. The latter is based on the Newton's equation of motion but including a rapidly fluctuating force, Gaussian distributed, representing the interaction among the particle and the solvent. It is well-known that in Euclidean open spaces the MSD calculated from the Langevin equation reproduces the standard Einstein kinematical relation. In this kind of spaces, both Langevin and diffusion equations describe the same dynamical behavior at the diffusive time regime, i.e., $t \gg \tau_B = M/\zeta$, where ζ is the friction coefficient of the solvent, M is the particle mass and τ_B the momentum relaxation time [24]. In fact, it is found that using methods of stochastic processes on manifolds, the diffusion equation can be derived from a Langevin-like equation [25]. Furthermore, Langevin-type equations have also been used to study Brownian motion in crystals with defects and including torsion effects [26], the lateral motion of proteins [27] and diffusion in fluctuating ruffled membranes [28].

In this work, we write the Langevin equation for manifolds without including torsion. Our starting point is the Newton's equation for free particles in a d-dimensional hypersurface. Free means here that particles do not interact between each other and non external force is acting on them, they are nevertheless restricted to move on the hypersurface. We find a set of equations that correspond to the global version of the equations found in reference [26]. The resulting equations allow us to study the curvature effects using the tools of the Riemann normal coordinates [29]. We reproduce the same leading curvature effects in the diffusion regime as in reference [22], but the Langevin equation also allows us to study shorter time regimes. Taking all this together, we investigate the particle dynamics for $\tau_{solvent} \ll t \ll \tau_B$, for $\tau_B \ll t < \tau_G$, as in reference [22], and for $t \gg \tau_G$. Here, $\tau_{solvent}$ is a characteristic time for the position and momentum relaxation of the solvent molecules, at which the Langevin description is not longer valid, and τ_G is the time scale thereafter the effects of the geometrical properties of the manifold become evident. We explicitly analyze the dynamics of particles confined along a circle, as well as on a sphere.

We test our predictions by means of Brownian dynamics computer simulations based on a heuristic adaptation of the Ermak-McCammon algorithm to the Langevin equation along curves, as well as on the standard algorithm, but for particles perpendicularly attached to the surface through a spring-like force. In the first case, which is here only applied to the circle, the particles are allowed to move in any direction with equal probability, but the geodesic distances they travel are Gaussian randomly distributed. In the second case, the particles are allowed to move everywhere in the $d+1$-dimensional Euclidean open space containing the hypersurface, but firmly attached to the latter by some kind of virtual springs acting perpendicularly to any point of the surface, at any time. In the limit case of very stiff springs, we get the same results from both routes, as we will see further below.

The manuscript is organized as follows. In section II we present the Langevin equation for curved manifolds, written in both local and global coordinates. In addition, we study the curvature effects on the MSD at the following regimes: $\tau_{solvent} \ll t \ll \tau_B$ and $\tau_B \ll t < \tau_G$. In section III we study the particle dynamics on the geometrical regime ($t \gg \tau_G$) by means of the diffusion equation on curved manifolds. In section IV we explicitly compare our predictions for particles restricted to move along a circle and on a sphere with Brownian dynamics computer simulations. Finally, in section V we summarize some concluding remarks and perspectives of our work.

II. LANGEVIN EQUATION ON CURVED MANIFOLDS

A. Global coordinates description

We now specify the basis of our Langevin dynamics formalism. It is defined over an Euclidean hypersurface $S \subset \mathbb{R}^{d+1}$, which is also defined as the points $\mathbf{X} \in \mathbb{R}^{d+1}$ such that $\Phi(\mathbf{X}) = 0$. The Langevin equation needs to include an holonomic constraint in order to bound a point particle to S.

Let us denote the momentum $\mathbf{P} \in T_{\mathbf{X}}(S)$, where $T_{\mathbf{X}}(S)$ is the tangent space at the point $\mathbf{X}$, and the position $\mathbf{X} \in \mathbb{R}^{d+1}$ of the particle. From a classical point of view, the addition of the term $\lambda\Phi(\mathbf{X})$ to the free-particle Lagrangian allows us to impose an holonomic constraint on S. Indeed, the equation of motion is $\dot{\mathbf{P}} = \lambda\, \nabla\Phi(\mathbf{X})$ and the required constraint is $\Phi(\mathbf{X}) = 0$. We should remark that $\lambda = 0$ relaxes the constraint. For the Langevin equation defined on S, we simply include the previous constraint, a friction term and a stochastic force

$$\dot{\mathbf{P}} = -\zeta\, \mathbf{P}/M + \lambda\, \nabla\Phi(\mathbf{X}) + \mathbf{f}(t) \quad (2)$$

$$\dot{\mathbf{X}} = \mathbf{P}/M, \quad (3)$$

$$\Phi(\mathbf{X}) = 0. \quad (4)$$

The second term of equation (2) represents the force caused by the holonomic constraint. The stochastic force $\mathbf{f}(t)$ is chosen such that it satisfies the fluctuation-dissipation relations

$$\langle f_i(t)\rangle = 0,$$
$$\langle f_i(t) f_j(t')\rangle = \Omega\delta_{ij}\delta(t-t'), \quad (5)$$

where $\langle\cdots\rangle$ stands for the average in the *ensemble* of field forces Gaussian distributed over $\mathbb{R}^{d+1}$ space (see Appendix A). $\mathbb{R}^{d+1}$ is a copy of $T_{\mathbf{X}}(S)\times\mathbb{R}$, i.e., the ensemble is given by all possible configurations of forces belonging to $\mathbb{R}^{d+1}$. In other words, for each point of the surface, we have a Gaussian distribution of forces.

The Lagrange multiplier λ can be obtained using the constraint (4) as follows. A time derivative on this constraint implies that

$$\nabla\Phi(\mathbf{X}) \cdot \mathbf{P} = 0, \quad (6)$$

where ∇ represents derivation in the space $\mathbb{R}^{d+1}$. Since the momentum $\mathbf{P} \in T_{\mathbf{X}}(S)$, then $\nabla\Phi$ is normal to the tangent space. Thus, the normal vector to the surface, i.e., normal to $T_{\mathbf{X}}(S)$, is given by $\mathbf{n} = \nabla\Phi(\mathbf{X}) / |\nabla\Phi(\mathbf{X})|$. Second derivative on equation (6) gives

$$\mathbf{n} \cdot \dot{\mathbf{P}} = -\frac{1}{M} P^i G_{ij} P^j, \tag{7}$$

with $G_{ij} = \partial_i \partial_j \Phi / |\nabla\Phi|$. Now, we get λ by equating (7) and the normal projection of (2). Then, $\lambda = -P^i G_{ij} P^j / M\,|\nabla\Phi| - \mathbf{n}\cdot\mathbf{f}/|\nabla\Phi|$. Therefore, the Langevin equation involves a non-linear term proportional to a second power in momenta,

$$\dot{\mathbf{P}} + \frac{1}{M} G_{ij} P^i P^j \mathbf{n} \;=\; -\frac{\zeta}{M}\,\mathbf{P} + \mathbb{P}(\mathbf{f}(t)), \tag{8}$$

where we have introduced a projector $\mathbb{P}$ that maps a vector $\mathbf{V} \in T_{\mathbf{X}}(S) \times \mathbb{R} \cong \mathbb{R}^{d+1}$ into the tangent space. This projector is given by $\mathbb{P}^{ij} = \delta^{ij} - n^i n^j$ and it satisfies the usual relationship: $\mathbb{P}^2 = \mathbb{P}$. The quadratic term in momenta is not a surprise since the left-hand side of equation (8) corresponds to the ordinary kinetic term for a particle over a hypersurface. In other words, the Langevin equation (8) reduces to the geodesic equation when both the friction and the stochastic force vanish. This will be clear further below when we write equation (8) in local coordinates.

We point out that the G matrix encodes the surface geometry. For instance, the constraint $\Phi(\mathbf{X}) = \mathbf{a}\cdot\mathbf{X} + b$ defines a plane in Euclidean space, where $\mathbf{a}$ is a constant vector and b a real number. In this particular case, the G matrix is zero and the normal vector of the surface is constant, $\mathbf{n} = \mathbf{a}/|\mathbf{a}|$, as it is required for a planar geometry. In the case of a sphere of radius R, we have $\Phi(\mathbf{X}) = \mathbf{X}^2/R^2 - 1$ and the normal vector satisfies $\mathbf{n} = \mathbf{X}/R$; the matrix G is given by $G_{ij} = \delta_{ij}/R$.

It is important to mention that the Langevin equation written in global coordinates (8) may be helpful for numerical simulations. Additionally, the global description is also the natural starting point to introduce ambient interactions, where the extrinsic geometry may play a role.

B. From a global to a local coordinates description

We now provide a local coordinates description of the Langevin equation (8). In local coordinates a hypersurface is parametrized by the mapping $\mathbf{X} : U \subset \mathbb{R}^2 \to S$, where a particular point in S is given by $p = \mathbf{X}(\xi^a)$, being ξ^a the local coordinates ($a = 1, \cdots, d$). In these coordinates, we have $\dot{\mathbf{X}} = \mathbf{e}_a \dot{\xi}^a$, $\mathbf{P} = \mathbf{e}_a p^a$, and $\mathbb{P}(\mathbf{f}) = \mathbf{e}_a f^a$, where $p^a = g^{ab} p_b$ is the local momentum and $\mathbf{e}_a = \partial_a \mathbf{X}$ the tangent vectors (note that $\partial_a = \partial/\partial\xi^a$). Thus, the first derivative of the momentum is given by

$$\dot{\mathbf{P}} \;=\; \frac{1}{M}\partial_b \mathbf{e}_a p^a p^b + \mathbf{e}_a \dot{p^a}, \tag{9}$$

where $\dot{p^a} \equiv d(g^{ab}p_b)/dt$. The partial derivative $\partial_b \mathbf{e}_a$ can be computed using the Weingarten-Gauss equations $\nabla_a \mathbf{e}_b = -K_{ab}\mathbf{n}$, where ∇_a is the covariant derivative, compatible with the metric g_{ab}, and K_{ab} the component of the second fundamental form [30]. The Weingarten-Gauss equations can be written in terms of the Christoffel symbols as $\partial_a \mathbf{e}_b = \Gamma^c{}_{ba}\mathbf{e}_c - K_{ba}\mathbf{n}$. By using this equation in the momentum time derivative we obtain

$$\dot{\mathbf{P}} = \left(\frac{1}{M}\Gamma^c{}_{ba} p^b p^a + \dot{p^c}\right)\mathbf{e}_c - \frac{1}{M} K_{ab} p^a p^b \mathbf{n}. \tag{10}$$

The local coordinates version of the Langevin equation can be straightforwardly obtained by substituting equation (10) in equation (8). Hence, the tangent projection takes the form,

$$\begin{aligned} \dot{p^c} \;&=\; -\frac{\zeta}{M} p^c - \frac{1}{M}\Gamma^c{}_{ba} p^b p^a + f^c, \\ \dot{\xi}^a \;&=\; g^{ab} p_b / M, \end{aligned} \tag{11}$$

while the normal projection is given by

$$K_{ab} = \mathbf{e}^i_a G_{ij} \mathbf{e}^j_b. \tag{12}$$

Equations (11) and (12) are the local version of the Langevin equation (8) and they can be easily extended to the case of manifolds with torsion (see [26]). As we mentioned above, the quadratic contribution in momenta is just the geodesic contribution. The normal projection provides a geometrical identity that allows us to derive the extrinsic curvature in terms of the G matrix. This identity is not casual; it is actually the same found at the level set formulation of the hypersurfaces geometry [30]. The extrinsic properties of the hypersurface are not playing a crucial role, as it is expected from the very beginning, since the motion of the particle intrinsically occur on the hypersurface.

Regarding the fluctuation-dissipation relations, the stochastic forces satisfy the following properties:

$$\begin{aligned} \langle f_a(t)\rangle \;&=\; 0, \\ \langle f_a(t) f_b(t')\rangle \;&=\; \Omega\delta_{ab}\delta(t-t'), \end{aligned} \tag{13}$$

where δ_{ab} is the two-dimensional Kronecker's delta. These relations are equivalent to their global version (see Appendix A).

C. Dynamics beyond a local neighborhood

Based on equation (11), it is clear that the particle dynamics does not depend on the extrinsic properties of the geometry. This means that the dynamics on a hypersurface can be studied in a Riemannian geometry, what we do in the following. Additionally, we mainly focus on the diffusion in the weak curvature regime. Let us recall that if $V \subset S$ is a local neighborhood of S, the map $\mathbf{X} : U \subset \mathbb{R}^d \to V$ is a local diffeomorphism [30],

then $V \equiv \mathbf{X}(U) \cong \mathbb{R}^d$. This implies that in a local neighborhood, we should have the same particle dynamics as found in planar spaces (see reference [24] for the $\mathbb{R}^3$ case). Thus, it makes sense to study curvature effects around the Euclidean solution.

In what follows, we first review the particle dynamics on the Euclidean geometry $S = \mathbb{R}^d$, i.e., when the curvature is zero, and, second, we expand the Euclidean solution in order to study the leading curvature effects on the particle dynamics over the surface.

1. *Euclidean geometry $S = \mathbb{R}^d$*

In the Euclidean geometry, both the global and local descriptions are the same; the Euclidean metric is simply $g_{ab} = \delta_{ab}$ and the Chrystoffel symbols are zero. In this case, the Langevin dynamics formalism reduces to the well-known standard equations [24]

$$\begin{aligned} \dot{p^c} &= -\frac{\zeta}{M} p^c + f^c, \\ \dot{\xi}^c &= \frac{1}{M} p^c, \end{aligned} \tag{14}$$

and their solution can be written as [24, 25],

$$\begin{aligned} p^c(t) &= p_0^c e^{-\frac{\zeta}{M}t} + \int_0^t dt' f^c(t') e^{-\frac{\zeta}{M}(t-t')}, \\ y^c(t) &= y_0^c + \frac{1}{M}\int_0^t dt' p^c(t'). \end{aligned} \tag{15}$$

Averaging equations (15) over the ensemble of stochastic forces, one easily obtains

$$\begin{aligned} \langle p^c(t) \rangle &= p_0^c e^{-\frac{\zeta}{M}t}, \\ \langle y^c(t) \rangle &= y_0^c + \frac{1}{\zeta} p_0^c \left(1 - e^{-\frac{\zeta}{M}t}\right). \end{aligned} \tag{16}$$

We observe that the mean momentum decreases exponentially with time (with the decaying time scale $\tau_B = M/\zeta$) and the particle position is shifted by $p^c(0)/\zeta$ at long-times.

We now consider for simplicity that $p_0^c = 0$ and $y_0^c = 0$. Other physical quantities of interest are both the mean quadratic momentum, i.e., $\langle p^c(t) p_c(t) \rangle$, and the mean square displacement, $s^2 = y^c y_c$. In order to calculate them, it is useful to find the temporal correlation function between two momenta, $p^a(t)$ and $p^b(t')$, at times t and t', given by (see Appendix B for further details)

$$\left\langle p^a(t) p^b(t') \right\rangle = \frac{M}{2\zeta} \Omega \delta^{ab} \left[e^{-\frac{\zeta}{M}|t-t'|} - e^{-\frac{\zeta}{M}(t+t')} \right]. \tag{17}$$

Using previous equation, it is straightforward to obtain the mean quadratic momentum:

$$\langle p^c(t) p_c(t) \rangle = \frac{d\Omega M}{2\zeta} \left(1 - e^{-2\frac{\zeta}{M}t}\right). \tag{18}$$

Proceeding along the same lines, we also get the MSD:

$$\left\langle s^2(t) \right\rangle = \frac{d\Omega M}{\zeta^3} \left[\frac{\zeta}{M} t - \frac{1}{2}(e^{-2\frac{\zeta}{M}t} - 1) - 2(1 - e^{-\frac{\zeta}{M}t}) \right]. \tag{19}$$

In the diffusive regime, $t \gg \tau_B$, the average kinetic energy reaches its equilibrium value. This allows the evaluation of Ω from the equipartition theorem. Thus, $\langle p^c(t) p_c(t) \rangle = dk_B T/2$ and $\Omega = 2\zeta k_B T$, where k_B is the Boltzmann constant and T the absolute temperature. We also observe that in this time regime the MSD reproduces the standard kinematical Einstein relation $\left\langle s^2(t) \right\rangle = 2dD_0 t$, where $D_0 = k_B T/\zeta$ is the free-particle diffusion coefficient [24]. We should point out that the value of Ω is independent of whether the space is curved or not, since it only depends on quantities intrinsic to the fluid, as solvent friction and particle dimension.

Higher order temporal correlation functions are also useful. In particular, we will see below that the four-points function $G^{abcd}(t_1, t_2, t_3, t_4) \equiv \left\langle p^a(t_1) p^b(t_2) p^c(t_3) p^d(t_4) \right\rangle$ is necessary in order to obtain the leading curvature corrections. This correlation function can be computed by using the Wick's theorem [25]:

$$\begin{aligned} G^{abcd}(t_1, t_2, t_3, t_4) &= \left\langle p^a(t_1) p^b(t_2) \right\rangle \left\langle p^c(t_3) p^d(t_4) \right\rangle \\ &+ \left\langle p^a(t_1) p^c(t_3) \right\rangle \left\langle p^b(t_3) p^d(t_4) \right\rangle \\ &+ \left\langle p^a(t_1) p^d(t_4) \right\rangle \left\langle p^b(t_2) p^c(t_3) \right\rangle \end{aligned} \tag{20}$$

2. *Leading weak curvature effects*

We turn now to the derivation of the leading weak curvature effects on the particles dynamics. As we already discussed, the Langevin equation is quadratic in the momentum and that contribution is coupled to the particles positions through the Chrystoffel symbols. The resulting equations are difficult to solve analytically, among other reasons because the left-hand side of equation (11) involves a temporal derivative of the metric. Using $p^a = g^{ab} p_b$ (p_a is independent of the metric), the local Langevin equation allows us to obtain the following expressions:

$$\begin{aligned} \dot{p_d} &= -\frac{\zeta}{M} p_d - \frac{1}{M} g_{cd} \left(\partial_a g^{cf}\right) g^{ab} p_b p_f \\ &\quad - \frac{1}{M} g_{cd} \Gamma^c{}_{ba} g^{bf} g^{ah} p_f p_h + f_d, \\ \dot{y^a} &= \frac{1}{M} g^{ab} p_b. \end{aligned} \tag{21}$$

In order to explore curvature effects, we expand equation (21) around the planar solution (15). To reach this goal, we use the Riemann normal coordinates [29]. In normal coordinates, we have

$$\begin{aligned} g^{ab} &= \delta^{ab} - \frac{1}{3} R^a{}_{cd}{}^b y^c y^d + O(y^3), \\ \Gamma^c{}_{ba} &= \frac{1}{3} \left(R^c{}_{bda} + R^c{}_{adb} \right) y^d + O(y^3), \end{aligned} \tag{22}$$

where $R^a{}_{bcd}$ are the components of the Riemann curvature tensor. Using (22) in (21) one obtains

$$\begin{aligned} \dot{p_d} &= -\frac{\zeta}{M}p_d - \frac{1}{3M}R_{dbfa}y^f p^b p^a + \cdots + f_d \\ \dot{y^a} &= \frac{1}{M}(\delta^{ab} - \frac{1}{3}R^a{}_{cd}{}^b y^c y^d + \cdots)p_b. \end{aligned} \tag{23}$$

We should notice that the Langevin equation in Euclidean geometries (14) is recovered when the curvature vanishes. In order to find a solution around the Euclidean case (15) we expand the momentum and position in the following way: $p_d = q_d + \delta q_d$ and $y^a = z^a + \delta z^a$, where q_d and z^a are the solutions for zero curvature, given by (15). Here, we have assumed that $\delta q = 0$ and $\delta z = 0$ when $R^a{}_{bcd} = 0$. If we consider only linear terms in curvature, we obtain the equation for δq_d:

$$\dot{\delta q_d} = -\frac{\zeta}{M}\delta q_d - \frac{1}{3M}R_{dbfa}z^f q^b q^a. \tag{24}$$

The second term of the right-hand side does not depend on δq; it depends only on time. The integration of equation (24) is similar to the one in the planar case. The initial condition for $\delta q_d(t)$ is $\delta q_d(0) = 0$, since $p_d(t)$ satisfies $p_d(0) = q_d(0)$. Therefore, the momentum, up to linear terms, in an arbitrary Riemannian geometry is given by

$$\begin{aligned} p_d(t) &= q_d(t) - \frac{1}{3M^2}R_{dbca}\int_0^{t'} dt' e^{-\frac{\zeta}{M}(t-t')} \\ &\quad \times \int_0^{t''} dt'' q^c(t'')q^b(t')q^a(t'), \end{aligned} \tag{25}$$

and the position, up to linear terms as well, takes the form

$$\begin{aligned} y^a(t) &= z^a(t) - \frac{1}{3M^3}R^a_{bcd}\int_0^t dt' \int_0^{t''} dt'' e^{-\frac{\zeta}{M}(t'-t'')} \\ &\quad \times \int_0^{t''} dt''' q^b(t'')q^c(t''')q^d(t''). \end{aligned} \tag{26}$$

Wick's theorem allows us to determine the temporal correlation functions of $q_a(t)$. Therefore, we have found that the odd correlations vanish, as in the case of the mean values of the momentum and position: $\langle p_a(t)\rangle = 0$ and $\langle y_a(t)\rangle = 0$. This means there is not preferential points on the surface and the mean values are independent of the geometry. This result may change however for non-zero initial conditions.

Up to linear terms in the curvature we obtain the following expectation value for $s^2(t)$:

$$\left\langle s^2(t)\right\rangle = \langle z^a(t)z_a(t)\rangle - \frac{1}{3M^4}R^a{}_{(ijk)}J_a{}^{ijk}(t) + \cdots, \tag{27}$$

where $\langle z^a(t)z_a(t)\rangle$ is the same as in equation (19), $R^a{}_{(ijk)} \equiv R^a{}_{ijk} + R^a{}_{kji}$ and

$$\begin{aligned} J_{aijk}(t) &= \int_0^t dt_1 \int_0^t dt_2 \int_0^{t_2} dt_3 \int_0^{t_3} dt_4 e^{-\frac{\zeta}{M}(t_2-t_3)} \\ &\quad \times G_{aijk}(t_1, t_3, t_4, t_3). \end{aligned} \tag{28}$$

The quantity $J_{aijk}(t)$ captures the dynamical contribution that appears in the weak curvature regime. In addition, the four-points correlation function G_{aijk} is defined according to equation (20); it is built by the products of two-point correlation functions and each of them carries a Kronecker's delta. Hence, using the symmetries of the Riemann tensor, the MSD reduces to

$$\left\langle s^2(t)\right\rangle = \langle z^a(t)z_a(t)\rangle - \frac{2R_g}{3}J(t) + \cdots, \tag{29}$$

where R_g is the scalar curvature and

$$\begin{aligned} J(t) &= \frac{1}{M^4}\int_0^t dt_1 \int_0^t dt_2 \int_0^{t_2} dt_3 \int_0^{t_3} dt_4 e^{-\frac{\zeta}{M}(t_2-t_3)} \\ &\quad \times \left(G(t_1,t_4)G(t_3,t_3) - G(t_1,t_3)G(t_4,t_3)\right). \end{aligned} \tag{30}$$

Equation (30) can be straightforwardly integrated (see Appendix B). Equation (29) represents the MSD (geodesic mean square displacement) in the weak curvature regime. As we can appreciate from equation (30), the time scale $\tau_B = M/\zeta$ defines two time regimes: The one with $t \ll \tau_B$ (but very much larger than $\tau_{solvent}$) or the ballistic regime, and the one with $t \gg \tau_B$ or the diffusive regime. In the first case, the MSD is given by

$$\left\langle s^2\left(t\right)\right\rangle \approx \frac{2d\zeta k_B T}{M^2}t^3. \tag{31}$$

The cubic term is the ordinary contribution to the ballistic regime when the initial condition is $p_0^c = 0$ (it becomes quadratic in t for non-zero initial conditions [24]). The next curvature contribution is of order t^6; typically negligible unless there is a region of very high curvature.

In the diffusive regime, $t \gg \tau_B$, the function $J\left(t\right)$ reduces to $J\left(t\right) \approx \left(D_0 t\right)^2$. Therefore, the MSD becomes

$$\left\langle s^2(t)\right\rangle = 2dD_0 t - \frac{2R_g}{3}\left(D_0 t\right)^2 + \cdots. \tag{32}$$

This result is the same found in reference [22] by means of the diffusion equation on curved manifolds. The MSD shows a deviation from the planar result due to curvature effects. Furthermore, equation (32) also shows the raise of two different diffusive regimes: The one with $\tau_B \ll t < \tau_G$, and the so-called long-time regime, also called geometric regime, $t \gg \tau_G$. Here, $\tau_G = 3d/\left|R_g\right| D_0$ stands for the time thereafter the curvature effects become dominant. Thus, up to linear order in the curvature, the Langevin equation and the diffusion equation are equivalent in the short-time diffusive regime. Nonetheless, additional curvature effects may be encoded in the Langevin equations for $t \gg \tau_G$, which we do not discern in this paper.

It is important to mention that in the planar case, i.e., $|R_g| \to 0$, the particle cannot feel any effect associated with the geometry (τ_G is never reached, then it grows towards infinity). Additionally, we should emphasize that in the particular case of $d = 1$ the MSD may exhibit deviations that cannot be associated to R_g, since

the Gaussian curvature of lines is zero. In fact, as we will see below, those effects are associated with the finite-size of the phase space.

From now on, we will consider that the complete diffusive regime is well described by both the Langevin equation and the diffusion equation. In the following section we discuss some properties of the diffusive motion of the particles along a circle, S^1, and on a sphere, S^2.

III. DIFFUSION IN S^1 AND S^2

We now choose the diffusion equation in order to study the geometric regime ($t \gg \tau_G$) in the manifolds S^1 and S^2 (for a discussion on the diffusion on arbitrary hyperspheres see, for example, reference [31]). The diffusion equation on curved manifolds can be written as [22],

$$\begin{aligned} \frac{\partial P(x,x',t)}{\partial t} &= D_0 \Delta_g P(x,x',t), \\ P(x,x',0) &= \frac{1}{\sqrt{g}}\delta^{(d)}(x-x'), \end{aligned} \tag{33}$$

where $P(x,x',t)\,dv$ is the probability of finding the diffusing particles in the volume element $dv = \sqrt{g}d^dx$, given that they began to move at x'. The probability density distribution $P(x,x',t)$ is normalized with respect to the volume v of the manifold and D_0 is the free-particle diffusion coefficient. The operator Δ_g, called the Laplace-Beltrami operator, is defined by

$$\Delta_g f = \frac{1}{\sqrt{g}}\partial_a\left(\sqrt{g}g^{ab}\partial_b f\right), \tag{34}$$

with $g = \det(g_{ab})$ and f is a scalar function. The geometry is coupled to the Brownian motion through the metric g. The diffusion equation (33) is the same as the heat kernel equation and it has a lot of applications in the context of field theories on curved spaces [32].

The expectation value of a scalar function $\mathcal{O}$ defined on the manifold is given in the standard fashion, i.e.,

$$\langle \mathcal{O}(x)\rangle = \int_{\mathbb{M}} dv\ \mathcal{O}(x)\,P(x,x',t), \tag{35}$$

and $\langle \mathcal{O}(x)\rangle$ depends on the initial point x'. The characteristics of observables in manifolds are related with the particular structure of $P(x,x',t)$. Furthermore, the probability density distribution $P(x,x',t)$ can be determined by solving the eigenvalue problem $-\Delta_g\Psi = E\Psi$, where E is the eigenvalue corresponding to the eigenfunction Ψ. In addition, it is known that for compact manifolds, the spectra of Δ_g is discrete and it can be written in a growing sequence $\{\lambda_0 = 0, \lambda_1, \lambda_2, \dots\}$, where $\lambda_{I+1} > \lambda_I$ [33]. We also have a sequence of orthogonal eigenfunction $\Psi_1, \Psi_2, \cdots$ in $L^2(S)$ (square-integrated functions of S). In this sense, the probability density distribution can be formally written as [34]

$$P(x,x',t) = \sum_I e^{-\lambda_I D_0 t}\Psi_I^*(x')\,\Psi_I(x), \tag{36}$$

with Ψ^* being the complex conjugate of Ψ. We note that degeneracy of eigenvalues is explicitly considered in the sum.

Now, let us consider an arbitrary observable $\mathcal{O}$. Its dynamical behavior can be obtained using the formal expression for $P(x,x',t)$. The expectation value $\langle \mathcal{O}(x)\rangle$ has a generic form; its structure around the geometric regime is determined by the smallest eigenvalues. Then, it can be written as follows:

$$\langle \mathcal{O}(x)\rangle \approx a_0 - a_1 e^{-D_0 t\lambda_1} + \cdots, \tag{37}$$

where $a_0 = \frac{1}{v}\int dv\mathcal{O}$ and $a_1 = \frac{1}{v}\int dv\ \Psi_1^*\mathcal{O}\Psi_1$.

We can easily obtain some properties of any observable by looking at the particular form of equation (37). For example, at long times it converges to the expectation value a_0. This is a consequence of the compactness of the manifold. In physical terms, the positions of the particles relax and their distribution does not longer evolve with time. The expectation value $\langle \mathcal{O}(x)\rangle$ becomes a_0 as a consequence of the finite size of the space. The quantity a_0 is the geometrical average of $\mathcal{O}$; this is the reason we called this regime the geometric regime. Although counterintuitive, the values of the observables do not depend on the temperature for $t \gg \tau_G$; it is only a function of the surface geometry.

A. Brownian motion over S^1

Brownian motion on the circle represents, after the motion on the straight line, the simplest example where there is a clear manifestation of the geometrical effects on the particle dynamics, but it is also the most fundamental one, since it is fully described by a single physical variable. It is also relevant for the theoretical and experimental study of single-file diffusion in quasi-one-dimensional interacting systems (see, e.g., [35] and references therein).

The circle is the mappping $\mathbf{X} : [0, 2\pi] \to \mathbb{R}^2$, where $\mathbf{X} = (R\cos\varphi, R\sin\varphi)$, with R being the circle radius. The Laplace-Beltrami operator in this case takes the form $\Delta_{S^1} = \frac{1}{R^2}\frac{\partial^2}{\partial\varphi^2}$. The eigenfunctions of this operator form the complete orthonormal set $\left\{e^{im\varphi} \mid m \in \mathbb{Z}\right\}$ in $L^2(S^1)$ and their corresponding eigenvalues are $\lambda_m = -m^2/R^2$.

In order to study Brownian motion on S^1, we choose the following initial and boundary conditions: $\varphi'(0) = 0$ and $P(\varphi, 0, 0) = \delta(\varphi)/2\pi R$. After some simplifications, the explicit solution of the diffusion equation is

$$P(\varphi,t) = \frac{1}{2\pi R}\left(1 + 2\sum_{m=1}^{\infty} e^{-m^2\frac{D_0 t}{R^2}}\cos(m\varphi)\right). \tag{38}$$

In this case, the distribution is normalized with the perimeter of the circle, i.e., $\int_I ds\ P(\varphi,t) = 1$, where $I = (-\pi, \pi)$ and $ds = R\ d\varphi$. The distribution is also symmetric under the interchange $\varphi \to -\varphi$.

The first moment, $\langle s(t)\rangle$, and the second moment or MSD, $\left\langle s^2(t)\right\rangle$, of the distribution can be straightfor-

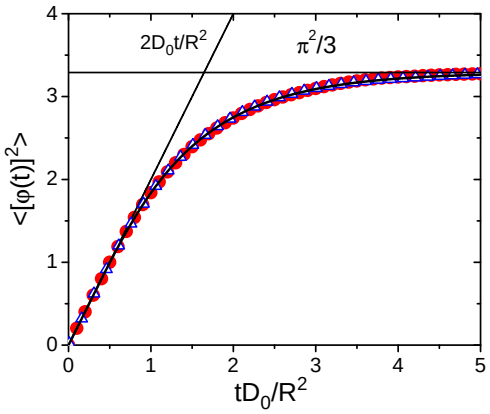

FIG. 1: Mean square angular displacement as a function of time for free Brownian particles diffusing along a circle. The line corresponds to our theoretical result given by equation (39), and the symbols to the Brownian computer simulations results obtained by means of both the standard Ermak and McCammon algorithm (circles) and its heuristic adaptation to curves (triangles). The error bars of the simulation data are smaller than the size of the symbols. There is no appreciable difference between the results. The straight lines stand for the short and long-time limits.

wardly evaluated. The former is zero, since the distribution is an even function, whereas the MSD has the form

$$\frac{\left\langle s^2(t)\right\rangle}{R^2} = \frac{\pi^2}{3} + 4\sum_{m=1}^{\infty}(-1)^m \frac{e^{-m^2\frac{D_0 t}{R^2}}}{m^2}, \qquad (39)$$

with $s = R\varphi$ being the arc-length. On the one hand, the MSD given by equation (39) reduces to $\left\langle s^2(t)\right\rangle = 2D_0 t$ for short times ($\tau_B \ll t \ll \tau_G$). On the other hand, at long times ($t \gg t_G = R^2/D_0$) we have $\left\langle s^2(t)\right\rangle = \pi^2 R^2/3$. In the geometric regime the dependence is only on the size of the circle. The numerical evaluation of equation (39) is shown in figure 1.

As we mentioned previously, although the MSD in (39) deviates from the planar result, this difference is due to the finite size of the circle and not to curvature effects. We compare the predictions of equation (39) with computer simulations in figure 1.

B. Brownian motion over S^2

Brownian dynamics on the sphere has been studied by several authors using different approaches [18, 19, 21, 36, 37]. However, our choose to define displacement as the geodesic distance between two points on the surface provides complementary information. Nevertheless, we do not discuss here the differences between alternative approximations. In contrast, we focus on the Brownian motion on the sphere in the framework of the diffusion equation (33).

The geometry of a sphere is encoded into the metric given by

$$ds^2 \equiv g_{ab}dx^a dx^b = R^2\left(d\theta^2 + \sin^2\theta d\varphi^2\right), \qquad (40)$$

where R, θ and φ are the radius, polar and azimuthal coordinates of the sphere, respectively. The Laplace-Beltrami operator on the sphere has eigenvalues and eigenvectors given by $\lambda_\ell = \ell(\ell+1)$ and $\{Y_{\ell m}(\theta,\varphi)\}$ with $\ell = 0,\cdots,\infty$ and $m = -\ell,\cdots,\ell$; $Y_{\ell m}(\theta,\varphi)$ being the standard spherical harmonics.

We choose x' to be on the north pole and take advantage of the rotational invariance. Besides, the boundary condition (33) is explicitly taken into account. The solution of the diffusion equation is then

$$P(\theta,t) = \sum_{\ell=0}^{\infty}\frac{2\ell+1}{4\pi R^2}\,P_\ell(\cos\theta)\exp\left[-\frac{D_0\ell(\ell+1)}{R^2}t\right], \qquad (41)$$

where P_ℓ is the Legendre polynomial of order ℓ. As in the previous case, we look for the information provided by $\langle s(t)\rangle$ and $\left\langle s^2(t)\right\rangle$, but we have now $s = R\theta$.

By means of the operator method defined in [22] it is possible to show that the short-time behavior of the MSD is given by equation (32) with the Gaussian curvature of the sphere, $R_g = 2/R^2$. It is interesting to note that the terms in the MSD that depend on the Gaussian curvature are always negative. This means that curvature effects only contribute to reduce the particle diffusion with time.

In the geometric regime, $t \gg \tau_G = 3R^2/D_0$, we get from equation (37)

$$\begin{aligned}\frac{\langle s\rangle}{R} &= \frac{\pi}{2}\left(1 - \frac{3}{4}e^{-2\frac{D_0 t}{R^2}} + \cdots\right)\\ \frac{\left\langle s^2\right\rangle}{R^2} &= \frac{\pi^2-4}{2}\left(1 - \frac{3\pi^2}{4\pi^2-16}e^{-2\frac{D_0 t}{R^2}} + \cdots\right).\end{aligned} \qquad (42)$$

At the beginning the particles move around their initial position, i.e., the north pole. After a long time, very much larger than τ_G, the expectation values $\langle s\rangle$ and $\left\langle s^2\right\rangle$ move towards the saturation values $\pi R/2$ and $(\pi^2-4)R^2/2$, respectively. The particle have visited all the points on the surface and confinement dominates entirely the diffusive behavior; the saturation values only depend on the size of the sphere. The numerical evaluation of equation (42) is shown in figure 2.

The expectation value of any observable $\mathcal{O} = \mathcal{O}(\theta,\varphi)$ on the sphere can be written as

$$\langle\mathcal{O}(\theta,\varphi)\rangle = \frac{R}{2}\sum_{\ell=0}^{\infty}(2\ell+1)\,g_{\mathcal{O}}(\ell)\,e^{-D_0\ell(\ell+1)t/R^2}, \qquad (43)$$

where $g_{\mathcal{O}}$ is the projection of $\mathcal{O}$ along the basis of Legendre polynomial. We explicitly show the functional form of $g_{\mathcal{O}}$ in Appendix C, for both g_s and g_{s^2}.

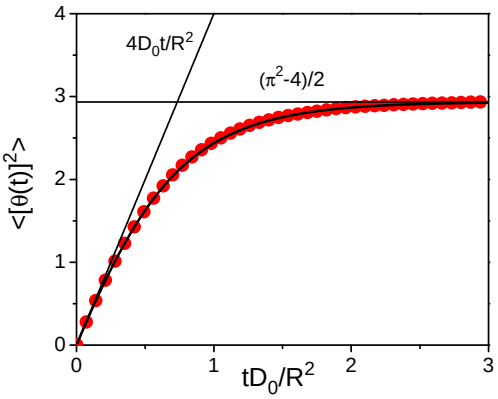

FIG. 2: Mean square polar angular displacement as a function of time for free Brownian particles diffusing over a sphere. The line correspond to our theoretical result given by equation (42), and the symbols to the Brownian computer simulations results obtained by means of the standard Ermak and McCammon algorithm (circles). The error bars of the simulation data are smaller than the size of the symbols. There is no appreciable difference between the results. The straight lines stand for the short and long-time limits.

IV. BROWNIAN DYNAMICS SIMULATIONS ON CURVED SURFACES

A. Standard Ermak and McCammon algorithm

In 1978, Ermak and McCammon introduced a method for simulating the Brownian dynamics of particles [38]. This method, which has been adapted in Euclidean coordinates, was derived from the Langevin equation and became consistent with the Fokker-Planck equation. Furthermore, such a method can be straightforwardly applied when either hydrodynamic interactions are considered explicitly or external forces act on the particles. This method has been successfully employed to study the structural and dynamic properties of a large variety of complex fluids, i.e., colloids, polymers, etc. [39]

The algorithm of Ermak and McCammon [38] is given by

$$\mathbf{X}_\alpha = \mathbf{X}^0_\alpha + \sum_{\beta=1}^{N} \frac{\partial \mathbf{D}^0_{\alpha\beta}}{\partial r_\beta}\Delta t + \sum_{\beta=1}^{N} \beta \mathbf{D}^0_{\alpha\beta}\mathbf{F}^0_\beta \Delta t + \delta\mathbf{X}_\alpha, \quad (44)$$

where N is the number of particles, $\beta = (k_B T)^{-1}$ is the inverse of the thermal energy, k_B being the Boltzmann constant and T the absolute temperature. The hydrodynamic interactions (HI) are included through the diffusion tensor $\mathbf{D}^0_{\alpha\beta}$, $\mathbf{F}^0_\beta$ is the total force exerted on the β-th particle and the index 0 tells us that the variable must be calculated at the beginning in time at every step. The term $\delta\mathbf{X}_\alpha$ represents a random displacement with a Gaussian distribution function with mean value zero and a covariance matrix given by the elements $\langle \delta X_{\alpha_i} \delta X_{\beta_j} \rangle = 2D^0_{\alpha_i\beta_j}\Delta t$; these are the requirements needed to satisfy the fluctuation-dissipation theorem (5). The indices α and β run over the particles, and the indices i and j over the cartesian coordinates. In our case, we do not consider HI and, therefore, $D^0_{\alpha_i\beta_j} = \delta_{ij}\delta_{\alpha\beta}D_0$, where D_0 is again the free-particle diffusion coefficient. With this assumption, the second term in the right-hand side of equation (44) disappears and allows us to simplify drastically the calculation of the third and fourth terms of the same side.

As we mentioned previously, the algorithm of Ermak and McCammon describes the temporal evolution of Euclidean variables. However, it can be still used to describe the dynamics of particles on curved surfaces. This can be done by considering an external force that constrains the movement of the particles on the surface. We demand that such a force does not contribute to the tangent displacements of the particles, i.e., this force has to act normal to any point of the manifold at any time to guarantee that it does not perform work on the system. Then, the simplest force that satisfies such requirements can be written as

$$\mathbf{F}_\alpha = -k(|\mathbf{X}_\alpha| - R)\mathbf{n}_\alpha, \quad (45)$$

where k is a spring-like constant, whose value is chosen in such a way that the particle displacements in the perpendicular direction to the surface is basically negligible, R is the radius of either the circle or the sphere and $\mathbf{n}_\alpha$ is a unit normal vector. Hence, equation (45) is incorporated in the standard algorithm for Brownian dynamics described in equation (44) to analyze the diffusion on the given surface.

We should mention that the addition of force (45) into equation (44) has the same effect on the particle dynamics as the second term of the left-hand side in equation (8), i.e., it only constrains the motion of the particles on the manifold. Thus, this kind of trick allows us to study the diffusion on curved surfaces through the use of the standard Ermak and McCammon algorithm.

B. Heuristic adaptation of the Ermak and McCammon algorithm to curves

Equation (44) takes the simple form $\mathbf{X}_\alpha = \mathbf{X}^0_\alpha + \delta\mathbf{X}_\alpha$ for free particles, with $\langle \delta X_{\alpha_i} \delta X_{\alpha_j} \rangle = 2\delta_{ij}D_0\Delta t$. In a d-dimensional Euclidian open space this process is equivalent to allow the particles to move in any direction with equal probability, as long as the distances they travel are Gaussian randomly distributed with variance $\langle \delta s_\alpha \delta s_\alpha \rangle = 2dD_0\Delta t$. This is however the short-time behavior of the MSD in d-dimensional manifolds (32). Hence, we heuristically extend the Ermak and McCammon algorithm to curved manifolds by allowing the particles to move in any direction with equal probability, but the geodesic distances they travel are Gaussian randomly

distributed, i.e., $s = s^0 + \delta s$ with $\langle \delta s \delta s \rangle = 2dD_0\Delta t$, as long as $\tau_B \ll \Delta t \ll \tau_G$.

In the particular case of a circle, this idea leads to the following algorithm: A uniform random number is generated in the interval $[0, 1]$; the particle in turn is allowed to move in the clock-wise direction if the result falls in $[0, 0.5]$, otherwise the particle moves in the opposite direction; a Gaussian randomly distributed number with variance $\langle \delta s \delta s \rangle = 2D_0\Delta t$ is then generated in order to determine the arc-length the particle travels; these steps are repeated for every particle, many times, in order to construct the dynamics of the system in its natural sequence. In our simulations, we let 1000 free particles to move in very short time steps, until they approximately cover a distance of 100 times the perimeter of the circle. The large number of particles allows to improve the numerical precision of our results.

We expect, on the one hand, the short-time behavior $\langle \Delta s^2(t) \rangle = 2D_0 t$, since this is included in the construction of the algorithm. On the other hand, for very long times ($t \gg \tau_G$) the particles has to distribute uniformly along the perimeter of the circle. Therefore, the geometric behavior of the MSD must be given by the simple average of the geodesic square displacement

$$\frac{\langle \Delta s^2(t \gg \tau_G) \rangle}{R^2} = \frac{1}{2\pi} \int_0^{2\pi} (\varphi - \langle \varphi \rangle)^2 d\varphi = \frac{\pi^2}{3}, \quad (46)$$

which agrees with equation (39). These and the intermediate values of $\langle \Delta s^2(t) \rangle$ are shown in figure 1.

The extension of these ideas to the general case of curved surfaces will be presented elsewhere.

V. CONCLUDING REMARKS AND PERSPECTIVES

In this work the diffusion of free particles on curved surfaces is studied. After writing the Langevin equation and the fluctuation-dissipation theorem for curved surfaces, we solved the former in the Riemann normal coordinates for weak curvatures, i.e., up to linear terms in the Riemann curvature tensor. From this solution, the dynamics of the particles can be clearly separated in three regimes; the ballistic one, $\tau_{solvent} \ll t \ll \tau_B$, and two diffusive regimes; short times, $\tau_B \ll t < \tau_G$, and long times, or geometric regime, $t \gg \tau_G$. No effects of the geometry were found, neither in the ballistic nor in the short-time diffusive regimes. We therefore conclude that the local dynamics occurs in the plane tangent to the surface. Nevertheless, in the long-time diffusive regime only the geometric effects take place. The free particle diffusion coefficient D_0 might be understood in terms of the short-time limit of the mean geodesic square displacement, $\langle \Delta s^2(\tau_B \ll t \ll \tau_G) \rangle = 2dD_0 t$, in a similar way as in the case of interacting particles. The geometry then appears as an external force acting on the diffusing particles, which can be recognized in the second term of the left side of equation (8).

We should remark that in the short-time diffusive regime the Langevin equation was found to have the same solution as the diffusion equation on curved surfaces [22]. We therefore used the latter in order to study the whole diffusive dynamics, although we do not discard the possibility to find differences between both equations beyond the weak curvature approximation. We particularly studied the diffusion of free particles along a circle, S^1, and on a sphere, S^2. We do not expect curvature effects in S^1 since its Gaussian curvature R_g is zero. However, the MSD displays a geometric diffusive regime due to confinement effects, since the particles are unable to move beyond the region were the circle is placed. In S^2 the confinement and curvature effects act together to define the geometrical regime. The difference between curvature and confinement effects is subtle and somehow counterintuitive. This will be carefully reported somewhere else.

In this work we also report some results from Brownian dynamics computer simulations. We obtained them by implementing the standard Ermak-McCammon algorithm, as well as its heuristic adaptation to curves. In the first case, we assumed that the particles are attached to the surface through springs acting on the particles everywhere, always perpendicularly to the surface. The spring constant was adjusted to guarantee the particle dynamics very close to the surface. In the second case, which was only applied to the circle, we allowed the particles to move in every direction along the curve, every time displacing geodesic lengths given by random Gaussian number with variance $\langle \delta s \delta s \rangle = 2dD_0\Delta t$, where $d = 1$ is the dimension of the circle. The quantitative comparison of the theoretical results with the simulation data is shown in figures 1 and 2.

A natural extension of this work could be the study of interacting particles. However, the interaction may produce colored distributions for the stochastic forces in the Langevin equation [40], so that Wick's theorem, which is of central importance in our calculations, were not longer valid. Nevertheless, it could be longer applied as an approximation, in the sense that the n-time correlation functions may be decomposed in terms of two-time correlation functions. In addition, both implementations of the Ermak and McCammon algorithm may be further used for interacting particles, as well as for other physical circumstances.

For instance, in the case of the sphere, let us think in a cylindrical Brownian particle located at its centre. Let us assume that the particle is fixed to that point, but free to rotate around it. The particle only feels the solvent in which it is suspended, i.e., the motion of the particle can be described by the rotational Langevin equation for free particles [41]. If we imagine a virtual straight line, coincident with the longitudinal axis of the cylinder, but extending its length indefinitely in both directions, then the points where this line cuts the surface of the sphere may display a motion equal to the one we are generating with our Brownian dynamics algorithms. Thus, the problem of the diffusion of free particles on a spherical

surface may be equivalent to the problem of the rotational diffusion of free particles. This equivalence could be extended to other surfaces, the circle for instance, as well as to the case of interacting particles. The latter including torques, which should be compatible with the interaction, given all particles are fixed to the centre of the sphere. No doubt that the study of this analogy is highly interesting.

Appendix A: Fluctuation-dissipation theorem

The stochastic force is Gaussian distributed for each point on the surface S. In global coordinates this distribution is given by [25]

$$d\mu = \prod_{i=1}^{3} [df_i] \exp\left\{ -\frac{1}{2\Omega} \int dt\ \delta^{ij} f_i f_j \right\}, \qquad \text{(A1)}$$

where $[df_i]$ is an appropiate functional measure. This is equivalent to a Gaussian vector field theory in one dimension. The expectation values are defined by $\langle \mathcal{O} \rangle = \int d\mu\ \mathcal{O} / \int d\mu$. In particular, the fluctuation-dissipation theorem (5) can be verified using (A1).

The force distribution (A1) also determines the fluctuaction-dissipation theorem in local coordinates (13). To show this, let us separate the force in tangent and normal components. Since, $\mathbf{e}_a$ and $\mathbf{n}$ are given for each point, thus $\mathbf{f} = \mathbf{e}^a f_a + \mathbf{n} f_n$ is a biyective transformation between $\{f_i\}$, with $i = 1, 2, 3$, and $\{f_a, f_n\}$, with $a = 1, 2$. Thus the measure $\prod_{i=1}^{3} [df_i]$ transforms to $\prod_{a=1}^{2} [df_a]\,[df_n]\,J$, where $J = \mathbf{n} \cdot (\mathbf{e}_1 \times \mathbf{e}_2)$ is the Jacobian. In addition, the argument of the Boltzmann weight can be splitted in these coordinates. Then, the measure $d\mu$ can be written as

$$d\mu = \prod_{a=1}^{2} [df_a]\,[df_n]\,J \exp\left\{ -\frac{1}{2\Omega} \int dt \left(g^{ab} f_a f_b + f_n^2 \right) \right\}. \qquad \text{(A2)}$$

Now, since the hypersurface is locally a plane we can always choose $\mathbf{e}_a$ such that $g_{ab} = \delta_{ab}$. Therefore, the local fluctuation-dissipation relations (13) can be straightforwardly obtained from (A1). This technical detail allows us to establish that both global and local versions of the Langevin equation on curved surfaces are equivalent.

Appendix B: Correlation functions

1. Green function

The correlation of two momenta for zero initial conditions can be computed from

$$\begin{aligned} \left\langle p^a(t)\, p^b(t') \right\rangle &= e^{-\frac{t+t'}{\tau_B}} \int_0^t dt_1 \int_0^{t'} dt_2 e^{-\frac{t_1+t_2}{\tau_B}} \\ &\times \left\langle f^a(t_1)\, f^b(t_2) \right\rangle. \end{aligned} \qquad \text{(B1)}$$

Next, we use the fluctuation-dissipation theorem (13). Thus the integration over variable t_2 leads to the following result

$$\int_0^{t'} dt_2 e^{t_2/\tau_B} \delta(t_2 - t_1) = \theta(t' - t_1)\, e^{t_1/\tau_B}, \qquad \text{(B2)}$$

where $\theta(x)$ is the Heaviside step-function. The remaining integral over t_1 can be done for two cases $t' > t$ and $t' < t$. If $t' > t$ then $t' > t_1$ for all $t_1 \in [0, t]$, therefore $\theta(t' - t_1) = 1$. Now, if $t' < t$ then the integration for t_1 can be splitted in two parts

$$\begin{aligned} \int_0^t dt_1 \theta(t' - t_1)\, e^{2t_1/\tau_B} &= \int_0^{t'} dt_1 \theta(t' - t_1)\, e^{2t_1/\tau_B} \\ &+ \int_{t'}^{t} dt_1 \theta(t' - t_1)\, e^{2t_1/\tau_B}. \end{aligned} \qquad \text{(B3)}$$

In the first integral $t' > t_1$, since $t_1 \in [0, t']$. Then for this integral $\theta(t' - t_1) = 1$. For the second integral, we have $t' < t_1$, since $t_1 \in [t', t]$. Therefore $\theta(t' - t_1) = 0$. Now, joining these results and performing the elementary integrals we reproduce equation (17).

2. Calculation of J function

The determination of $J(t)$ can be obtained from the calculation of

$$\begin{aligned} J(t) &= \frac{1}{M^4} \int_0^t dt_1 \int_0^t dt_2 \int_0^{t_2} dt_3 \int_0^{t_3} dt_4 e^{-\frac{1}{\tau_B}(t_2 - t_3)} \\ &\times \left(G(t_1, t_4) G(t_3, t_3) - G(t_1, t_3) G(t_4, t_3) \right). \end{aligned} \qquad \text{(B4)}$$

We should remark that the integral $I(t, \tau') = \int_0^t d\tau G(\tau, \tau')$ appears in various places in the multiple integral (B4). Thus, the function (B4) can be written as follows

$$\begin{aligned} J(t) &= \frac{1}{M^4} \int_0^t dt_2 \int_0^{t_2} dt_3 e^{-\frac{1}{\tau_B}(t_2 - t_3)} \\ &\times \left(G(t_3, t_3) \int_0^{t_3} dt_4 I(t, t_4) - I(t, t_3) I(t_3, t_3) \right). \end{aligned} \qquad \text{(B5)}$$

The advantage to write $J(t)$ in terms of $I(t,\tau')$ is that $\tau' \leq t$. For the calculation of the function $I(t,\tau')$ it is convenient to use the following equivalent expression for the Green function

$$G(t,t') = \tau_B\Omega\left[e^{-\frac{t}{\tau_B}}\theta(t-t')\sinh\frac{t'}{\tau_B} + e^{-\frac{t'}{\tau_B}}\theta(t'-t)\sinh\frac{t}{\tau_B}\right]. \quad \text{(B6)}$$

Performing its integral we obtain

$$I(t,\tau') = \frac{\tau_B^2\Omega}{2}e^{-\frac{1}{\tau_B}(t+\tau')}\left(1-e^{\frac{\tau'}{\tau_B}}\right) \times \left(1-2e^{\frac{t}{\tau_B}}+e^{\frac{\tau'}{\tau_B}}\right). \quad \text{(B7)}$$

Now, we carry out the elementary integrations involved in $(B5)$. We then get the following expression

$$J(t) = \frac{1}{6}(\tau_B D)^2\left\{e^{-\frac{t}{\tau_B}}\left[8+e^{-3\frac{t}{\tau_B}}-8e^{-2\frac{t}{\tau_B}}+36e^{-\frac{t}{\tau_B}} + 48\frac{t}{\tau_B}+e^{\frac{t}{\tau_B}}\left(-37+12\frac{t}{\tau_B}\right)\right]+e^{-4\frac{t}{\tau_B}}\left[1+e^{\frac{t}{\tau_B}}\right. \times \left(-8+e^{\frac{t}{\tau_B}}\left(15-40e^{\frac{t}{\tau_B}}-6\frac{t}{\tau_B}+e^{2\frac{t}{\tau_B}}(32 + 6\frac{t}{\tau_B}\left(\frac{t}{\tau_B}-4\right)\right)\right)\right)\left.\right]\right\}. \quad \text{(B8)}$$

Appendix C: Expectation values for Brownian motion over S^2

The expectation values for $\mathcal{O}=\mathcal{O}(\theta,\varphi)$ can be calculated from

$$\langle\mathcal{O}(\theta,\varphi)\rangle = \frac{R}{2}\sum_{\ell=0}^{\infty}(2\ell+1)\,g_{\mathcal{O}}(\ell)\,e^{-D\ell(\ell+1)t/R^2}, \quad \text{(C1)}$$

where

$$g_{\mathcal{O}}(\ell) = \int_0^{\pi}\int_0^{2\pi}d\theta d\varphi\sin\theta\;\mathcal{O}(\theta,\varphi)\,P_\ell(\cos\theta). \quad \text{(C2)}$$

Equation (C2) depends explicitly on the chosen form of $\mathcal{O}$. In general, equation (C1) cannot be written in a closed form and it must be studied numerically. In particular, we discuss here the mean values of the functions $\mathcal{O}=s=R\theta$, and $\mathcal{O}=s^2$. In order to have a more manageable form for these expectation values we use the following identity

$$P_\ell(\cos\theta) = (-1)^\ell\sum_{k=0}^{\ell}\binom{-\frac{1}{2}}{\ell}\binom{-\frac{1}{2}}{\ell-k}\cos\left[(\ell-2k)\,\theta\right]. \quad \text{(C3)}$$

Now, in order to obtain (C2) we perform the integration for even and odd vaues of ℓ. After performing the elementary integrations, we obtain the following results. For $s=R\theta$, $g_s(\ell)$ is zero for even values of ℓ, and for odd values of ℓ it takes the form

$$g_s(2p+1) = \frac{\pi}{2}\binom{-\frac{1}{2}}{p}\binom{-\frac{1}{2}}{p+1} - \pi\sum_{k=0}^{2p+1}\frac{\binom{-\frac{1}{2}}{k}\binom{-\frac{1}{2}}{2p+1-k}}{(2(p-k)+1)^2-1}, \quad \text{(C4)}$$

where the last sum does not take the values $k=p$ and $k=p+1$. For $s^2=R^2\theta^2$, it is not difficult to show the identity $g_{s^2}(2p+1)=\pi g_s(2p+1)$ for odd values of ℓ. However, for even values of ℓ we find

$$g_{s^2}(2p) = \sum_{k=0}^{2p}\binom{-\frac{1}{2}}{k}\binom{-\frac{1}{2}}{2p+1-k}H(2(p-k)), \quad \text{(C5)}$$

where H is a function defined as

$$H(z) \equiv \frac{12z^2+4-\pi^2\left(z^2-1\right)^2}{\left(z^2-1\right)^3},$$

and

$$\binom{x}{n} = x(x-1)(x-2)\cdots(x-n+1)/n!$$

is the binomial coefficient [42].

Acknowledgments

Financial support by PIFI-2011, PIEC, PROMEP (1035/08/3291), and CONACyT (through grants 61418/2007, 102339/2008, 60595 and the Red Temática de la Materia Condensada Blanda) is kindly acknowledged.

[1] E. Frey and K. Kroy, Annalen der Physik, **14**, 2050 (2005).

[2] Bei Lok Hu and Enric Verdaguer, Living Rev. Relativity, **11**, 3 (2008) .

[3] Benjamin Svetitsky, Phys. Rev. D **37**, 2484 (1988)

[4] Jörn Dunkel, Peter Hänggi, Physics Reports **471**, 1-73 (2009).

[5] Nina Malchus and Matthias Weiss, Biophysical Journal, **99**, 1321 (2010); Matthias Weiss, Hitoshi Hashimoto, and Tommy Nilsson, Biophysical Journal **84**, 4043 (2003); Valerii M. Sukhorukov, Jürgen Bereiter-Hahn, PLoS **4** e4604 (2009) .

[6] Bruce Alberts, Alexander Johnson, Julian Lewis, Martin Raff, Keith Roberts, and Peter Walter, *Molecular Biology of the Cell*, 4th edition *Garland Science* (2002).

[7] F. Córdoba-Valdés, C. Fleck and R. Castañeda-Priego, Rev. Mex. Fis. **53**, 475 (2007); F. Córdoba-Valdés, C. Fleck, J. Timmer and R. Castañeda-Priego, *submitted*.

[8] Ali Naji, Paul J. Atzberger, and Frank L. H. Brown, Phys. Rev. Lett. **102** ,138102 (2009).

[9] Faraudo J, J. Chem. Phys. **116**, 5831 (2002).

[10] Reister E and Seifert U, Europhys Lett. **71**, 859 (2005)

[11] Ali Naji, Paul J. Atzberger, and Frank L. H. Brown, Phys. Rev. Lett. **102**, 138102 (2009).

[12] Ellen Reister-Gottfried, Stefan M. Leitenberger, and Udo Seifert, Phys. Rev. E **81**, 031903 (2010).

[13] N. S. Gov, Phys. Rev. E **73**, 041918 (2006).

[14] Naohisa Ogawa, Phys. Rev. E **81**, 061113 (2010)

[15] Boris M. Aizenbud and Nahum D. Gershon, Biophys. J. **38**, 287 (1982).

[16] S. Gustafsson and B. Halle, J. Chem. Phys. **106**, 1880 (1997).

[17] D. Anderson and H. Wennerström, J. Phys. Chem. **94**, p. 8683 (1990).

[18] J. Balakrishnan, Phys. Rev. E **61**, 4648 (2000)

[19] R. Holyst, D. Plewczynski, A. Aksimentiev, and K. Burdzy, Phys. Rev. E **60**, 302 (1999).

[20] Micheal Christensen, Journal of Computational Physics **201**, 421-438 (2004).

[21] Tomoyoshi Yoshigaki, Phys. Rev. E **75**, 041901 (2007).

[22] Pavel Castro-Villarreal, J. Stat. Mech. P08006 (2010).

[23] Matteo Smerlak, New Journal of Phys. **14**, 023019 (2012); Matteo Smerlak, Phys. Rev. E **85**, 041134 (2012).

[24] J. K. G. Dhont, *An introdution to dynamics of colloids*, Ed. Elsevier, (1996).

[25] Jean Zinn-Justin, *Quantum Field Theory and Critical Phenomena*, 3rd Ed. Oxford (1995).

[26] H. Kleinert and S. V. Shabanov, J. Phys. A: Math. Gen. **31**, 7005-7009 (1998).

[27] Ellen Reister-Gottfried, Stefan M. Leitenberger, and Udo Seifert, Phys. Rev. E **75**, 011908 (2007)

[28] Ali Naji, and Franck L. H. Brown, J. Chem. Phys. **126**, 235103 (2007)

[29] Müller U, Schubert C, and van de Ven A E M, Gen. Rel. Grav. **31**, 1759 (1999).

[30] M. Spivak, *A Comprehensive Introduction to Differential Geometry* Vol. 3, 3rd Ed. 1999.

[31] Jean-Michel Caillol, Phys. A: Math. Gen. **37**, 3077-3083 (2004).

[32] D. V. Vassilevich, Phys. Rep. **388**, 279 (2003).

[33] I. Chavel, *Eigenvalues in Riemannian geometries* (Academic Press, 1984)

[34] Grugor'yan A, London Mathematical Society Lecture Note Series **273**, 140 (1999).

[35] S. Herrera-Velarde, A. Zamudio-Ojeda and R. Castañeda-Priego, J. Chem. Phys. **133**, 114912 (2010).

[36] Faraudo J, J. Chem. Phys. **116**, 5831 (2002).

[37] Radu P. Mondescu and M. Muthukumar, Phys. Rev E **57**, 4411 (1998).

[38] Donald L. Ermak and J. A. McCammon, J. Chem. Phys. **69**, 1352 (1978).

[39] Tri T. Pham, Ulf D. Schiller, J. Ravi Prakash, and B. Dünweg, J. Chem. Phys. **131**, 164114 (2009).

[40] M. Medina-Noyola, Faraday Discuss. Chem. Soc. **83**, 21 (1987).

[41] Th. Kirchhoff, H. Löwen, and R. Klein, Phys. Rev. E **53**, 5011 (1996).

[42] Gradshteyn and Ryzhik's, *Table of Integrals, Series, and Products Academic press* Seventh edition (Feb 2007)